Defining Navigation Requirements for Future Precision Lander Missions

Alicia Dwyer Cianciolo,[1] and Scott Striepe[2]
NASA Langley Research Center, Hampton, Virginia, 23681, USA

John Carson,[3] Ron Sostaric,[4] David Woffinden,[5]
NASA Johnson Space Center, Houston, TX, 77058, USA

and
Chris Karlgaard,[6] Rafael Lugo,[7] Richard Powell,[8] Jake Tynis[9]
Analytical Mechanics Associates, Hampton, Virginia, 23681, USA

Human mission concepts for both the Moon and Mars require landing precision capabilities beyond the current state of art. The Safe and Precise Landing Integrated Capabilities Evolution (SPLICE) project leverages previous work at NASA to develop multi-mission precision landing and hazard avoidance (PL&HA) technologies to meet the advanced landing requirements. SPLICE aims to develop guidance, navigation and control (GN&C) capabilities for both Moon and Mars lander missions. The approach the project is using to identify a standard suite begins with developing a PL&HA requirements matrix to inform technology investments. The approach to develop a multi-mission navigation requirements matrix includes identifying representative concepts of operations for both robotic and human missions. It also identifies navigation sensor options with estimated performance parameters. This paper summarizes the concepts of operations and sensors considered to develop the SPLICE PL&HA requirements matrix. A description of the analysis used to determine candidate optimal sensor suites and initial results are provided.

I. Introduction

Precision landing and hazard avoidance (PL&HA) requires a suite of technologies including sensors, algorithms and avionic components. Earth bound assets enjoy the luxury of a global positioning system not afforded to Lunar and Mars landers. As concepts evolve for human missions to both remote destinations, it is evident that the landing precision requirements exceed the current state of art. Over the past decade, NASA has invested in several efforts to develop, test, and infuse PL&HA technologies [1, 2]. The most recent effort, initiated in fiscal year 2018, is called Safe and Precise Landing Integrated Capabilities Evolution (SPLICE) [3]. SPLICE leverages previous work to develop multi-mission PL&HA technologies as part of a standard suite of guidance, navigation, and control (GN&C) capabilities for lander missions. The approach used to identify a standard suite starts with developing a multi-mission PL&HA requirements matrix to inform technology investments, then prioritizing those technology developments for infusion into near-term robotic missions, and finally promoting near-term robotic technologies that steer long-term human-mission capabilities. This document summarizes the process used to develop a multi-mission PL&HA requirements matrix.

The SPLICE approach to developing a multi-mission PL&HA requirements matrix considers multiple concepts of operations and sensor suites. First, concepts of operations for missions with precision landing requirements are

[1] Aerospace Engineer, Atmospheric Flight and Entry Systems Branch, AIAA Senior Member.
[2] Aerospace Engineer, Atmospheric Flight and Entry Systems Branch.
[3] SPLICE Project Manager (PM), AIAA Associate Fellow.
[4] SPLICE Deputy PM, AIAA Senior Member.
[5] Aerospace Engineer, GN&C Autonomous Flight Systems Branch, Aeroscience and Flight Mechanics Division.
[6] Supervising Engineer, Atmospheric Flight and Entry Systems Branch, AIAA Senior Member.
[7] Aerospace Engineer, Atmospheric Flight and Entry Systems Branch, AIAA Member.
[8] Aerospace Engineer, Analytical Mechanics Associates, AIAA Fellow.
[9] Aerospace Engineer, Atmospheric Flight and Entry Systems Branch, AIAA Member.

identified. The missions include multiple classes (e.g. robotic and human scale) and destinations (e.g. Moon, Mars, Europa). Reference trajectories are developed for each concept of operations. Then navigation sensors are identified. Individual sensors have a range of specifications that represent increments in cost or complexity. Therefore, it is desirable to consider combinations of sensors to determine which meet the PL&HA requirements. Initially, screening methods are used to determine the most feasible combinations of sensors and performance levels. The top sensor combinations are then implemented into a six-degree-of-freedom (6DOF) trajectory simulation for verification and detailed performance evaluation in the presence of full environmental dispersions. At the time of publication, the SPLICE PL&HA requirement matrix effort has completed the initial screening of select sensors for a single concept of operations. The objective is to identify the sensors that meet PL&HA requirements and are common across multiple missions. Those sensors will be recommended for investment and infusion on near term missions and will steer long-term human mission capabilities.

Section II describes representative concepts of operations for both robotic and human scale missions. Select navigation sensors options and performance parameters are presented in Section III. Section IV summarizes two screening tools used to evaluate sensor suite combinations. Section V illustrates the process by presenting the results of the initial screening of a specific mission concept of operations. Finally, sensor suites that meet all PL&HA landing criteria for the selected mission are described.

II. Concepts of Operations Summary

While each mission has unique navigation and PL&HA requirements, seven concepts of operations have been identified that have a broad range of sensor performance criteria. The goal of the study is to determine commonalities in sensor combinations needed to meet navigation requirements for precision landing across multiple concepts of operations. Based on the 2010 Decadal Survey [4] and the recent Space Directive 1 [5], three destinations are considered: The Moon, Mars, and Europa. To understand the range of PL&HA requirements needed, both robotic and human scale mission concepts are considered for the Moon and Mars. Table 1 provides the mission names, class, and destination of the concepts of operations being considered for this study.

Table 1. SPLICE concepts of operations used to define the PL&HA requirements matrix.

	Moon		Mars		Europa
	Equatorial	**Polar**			
Robotic	Merriam	Merriam	Mars Sample Return		Europa Lander
Human		ALHAT/ALTAIR	Mid L/D	Low L/D	

General PL&HA ground rules and assumptions are leveraged on all missions, namely that the vehicles must be delivered to within 50 m radius (3σ) of a specified landing target. One motivation for this targeting constraint is the fact that future missions may require delivery of multiple landers to the same landing zone. Based on past human lunar missions, the vertical and horizontal velocities at touchdown must be less than 2.0 m/s and less than 1 m/s (3σ) respectively. Vehicle attitude must be within +6 deg (3σ) and the attitude rates within 2 deg/s (3σ) in all axes. The study does not consider a vehicle azimuth pointing angle constraint at touchdown, typically required for sun pointing or communication and telecom reasons, since this is achievable without major performance impact to the GN&C design. Another general requirement is to minimize propellant use. Details of each concept of operations are presented in the following subsections.

A. Lunar Robotic Missions – Merriam lander

As a result of NASA's recent pivot to the Moon and plans for a robotic mission in the early 2020's, the first concept of operations describes a 300 kg payload class robotic lunar lander, denoted as the Merriam lander. The concept of operations starts in an initial 100 km circular low lunar polar orbit. The vehicle is assumed to have an initial mass of 2000 kg. A single solid rocket motor provides a maximum of 5000 N of thrust for the breaking burn to deorbit. Figure 1 shows the notional concept of operations. The landing site is arbitrarily selected to be 27.1° N latitude, 9.1° E longitude.

The vehicle uses three powered flight phases to achieve precision landing. The first is called powered descent initiation (PDI). This phase, which starts at perilune of 15 km, uses an Apollo-like landing guidance algorithm. The algorithm targets a 500 m slant range at 60deg line-of-sight at 250 m downrange of landing site when the vehicle has an altitude of approximately 430 m. Slant range is defined as the distance from the vehicle center of gravity to the target landing location. The algorithm also targets the vehicle velocity relative to the landing site to be -15m/s vertical,

30 m/s horizontal at that point in the trajectory and acceleration targets are 0 m/s^2 vertical, -3.5 m/s^2 horizontal. Once the vehicle reaches the 500 m slant range point, the second phase of flight, called the approach phase, begins.

With a 500 m slant range and 60 deg line-of-sight the Apollo guidance now targets a position with respect to the landing site of 0 m downrange of landing site, 50 m altitude. The velocity targets in the approach phase are -1.1m/s vertical, 0m/s horizontal and the acceleration targets are 0 m/s^2 in all axes. The final powered descent phase is the vertical phase that starts at 50 m above the landing site. Position targets for this phase are 0 m downrange of landing site, 2 m altitude. The velocity and acceleration, with respect to the landing site, are 0 m/s and 0 m/s^2 respectively in all axes. An illustration of the powered descent phases is shown in Fig. 2. To examine the effect of changing lighting conditions on the sensor suite, both equatorial and polar initial orbits are considered.

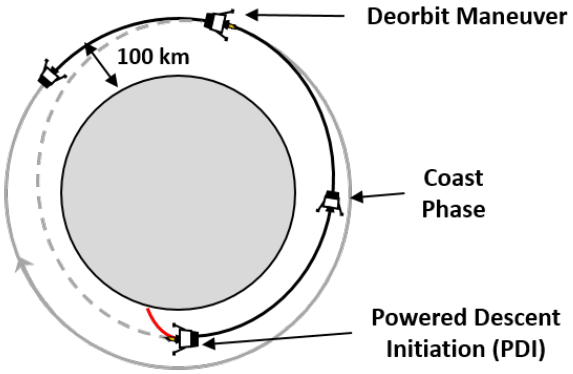

Figure 1. Notional lunar robotic initial orbit.

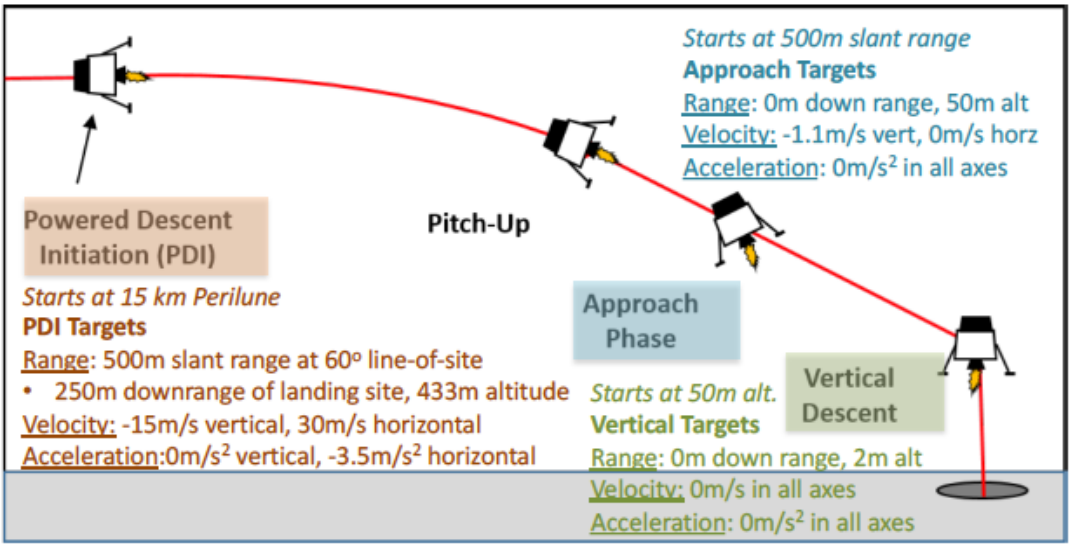

Figure 2. Lunar robotic descent concept of operations.

B. Lunar Human Mission

The reference concept of operations for the lunar human missions is derived from NASA's Altair mission concepts that use Autonomous Landing and Hazard Avoidance Technology (ALHAT) [1,6,7,8]. The ALHAT human scale mission assumes delivery of a 31t vehicle to a 100 km circular low lunar orbit, executes a de-orbit burn, and coasts to the PDI point. Prior to PDI, the ALHAT laser altimeter begins operation at 20 km altitude, as shown in Fig. 3. PDI occurs at about 15 km altitude, at a relative velocity of about 1700 m/s. Terrain Relative Navigation (TRN) operation begins at PDI and continues until 5 km altitude. In the ALHAT concept, the velocimeter begins operation at 2 km altitude. (Note that the current Navigation Doppler Lidar is capable of providing velocimetry at slant ranges of 7 km at the Moon). A pitch-up maneuver is initiated at 120 sec prior to landing. Following the completion of pitch-up is the Approach Phase, during which Hazard Detection and Avoidance (HDA) is performed. The concept of operations is similar to the robotic mission in the general multi-phase landing approach. However, the primary difference from is that the human trajectory design is chosen to minimize the attitude maneuvering during the hazard detection (HD) scan following the pitch-up maneuver. The final phase, Terminal Descent, is nominally a vertical descent to the landing site from 30 m altitude to touchdown, at a velocity of 1 m/s downward and near zero horizontal velocity.

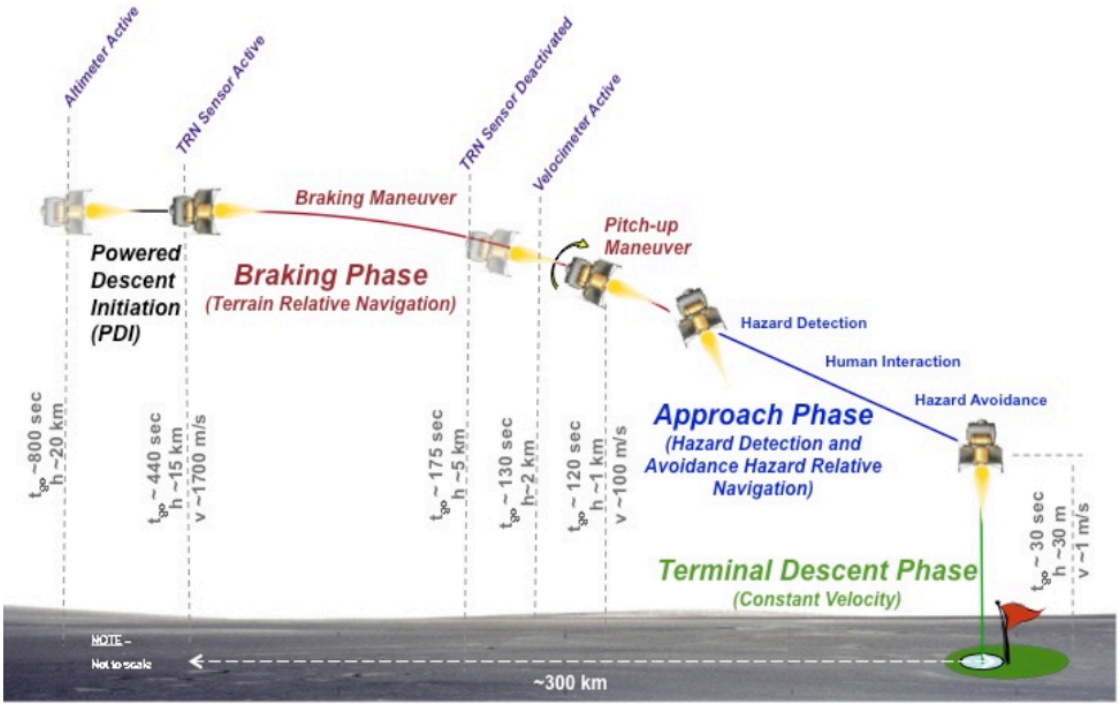

Figure 3. Notional human scale lunar mission concept of operations. [8]

C. Mars Robotic Mission

The Mars Sample Return lander provides a large robotic mission example. However, since the mission architecture has yet to be defined, the Mars Science Laboratory nominal concept of operations is used. The concept assumes a direct entry at Mars of a 3500 kg entry vehicle. The mission jettisons tungsten to change the center of gravity from a ballistic entry to achieve desired lift-to-drag (L/D) of 0.24 for entry and uses Reaction Control thrusters to bank the vehicle to steer to a desired landing spot. The entry guidance algorithm is also a modified Apollo entry algorithm. A supersonic parachute slows the vehicle during descent and a sky-crane maneuver is used to lower the rover to the surface. While the Mars 2020 will include a range trigger that will effectively reduce the landing ellipse to 12 x 8.5 km, additional sensors, and potentially changes to the concept of operations (to eliminate the parachute) are needed to achieve landing accuracies on the order of 50 m, which will be defined by the SPLICE screening process. Figure 4 shows the concept of operations for the Mars Science Laboratory mission.

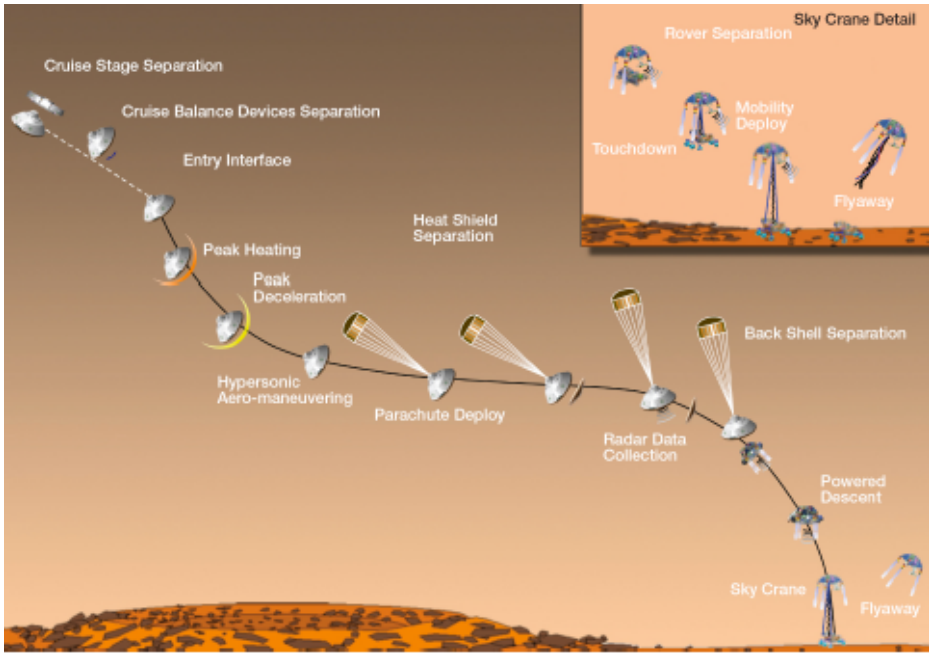

Figure 4. MSL EDL concept of operations [9]

D. Mars Human Scale Mission – Low L/D Vehicle

Less traditional approaches are considered to deliver human scale payload masses to the surface of Mars. One Low L/D (L/D~0.2) vehicle concept considered utilizes light-weight inflatable structures, such as the Hypersonic Inflatable Aerodynamic Decelerator (HIAD), to increase the vehicle drag diameter beyond the limitations of the launch vehicle. Recent studies have shown that a 16 m diameter HIAD has sufficient flight performance to deliver 20 metric ton payloads to the surface. The HIAD concept of operations is shown in Fig. 5. The Entry, Descent and Landing Architecture Study [10] has evaluated a HIAD concept that enters from a 1 Sol (33,800x 250 km) orbit. Because the human Mars architecture requires multiple landers to be delivered to the same 10km x 6 km landing zone, no jettison events are allowed during EDL to minimize risk of impacting a landed asset. Likewise, the use of tungsten to achieve the desired L/D and parachutes are not feasible for vehicles this size. Therefore, the desired lift is achieved by using articulating flaps and the descent deceleration is achieved using propulsion initiated at supersonic speeds, approximately Mach 3. Using supersonic retropropulsion has a significant impact on vehicle trajectory geometry and, thus, sensor performance. Details of the impact are described in Section II.G.

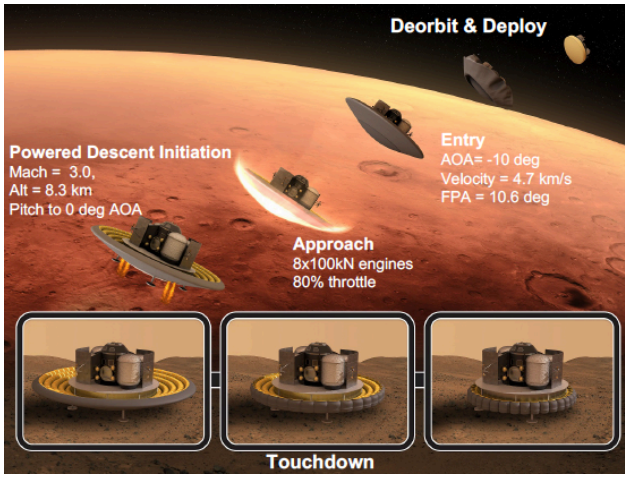

Figure 5. HIAD EDL concept of operations.[10]

E. Mars Human Scale Mission – Mid L/D Vehicle

A second concept of operations for human scale Mars landers is the Mid L/D concept[11,12]. This vehicle, with an L/D of 0.5, flies very different trajectory from the Low L/D concept and therefore offers different PL&HA sensor challenges. Like the HIAD, this vehicle concept of operations initiates from a 1 Sol orbit. The vehicle, 20 m x 8 m, has an entry angle of attack near 55 deg. At approximately 3.2 km and Mach of 2, the vehicle initiates eight engines for powered descent and the vehicle pitches to 90 degrees for a horizontal landing. Figure 6 shows the concept of operations for the Mid L/D vehicle. Like the Low L/D vehicle, a summary of the human Mars architecture that drove the Mid L/D EDL design is summarized in Ref [13].

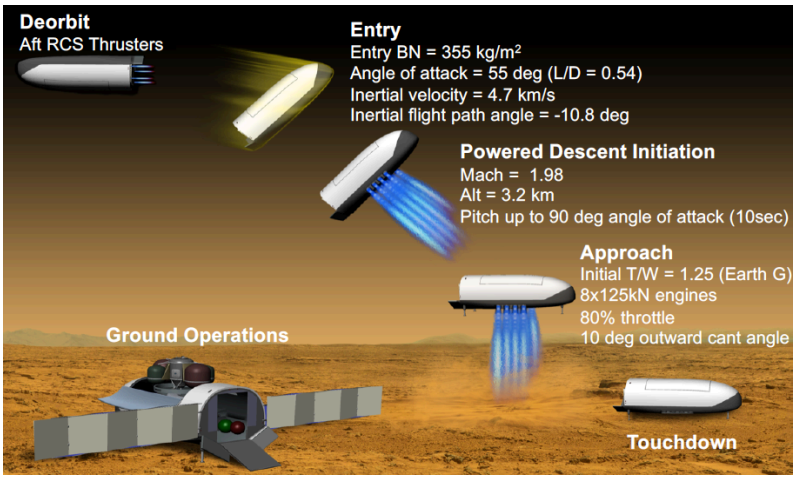

Figure 6. MID L/D vehicle EDL concept of operations. [11]

F. Europa Robotic Mission

The final concept of operations considered for the SPLICE PL&HA sensor suite analysis is the Europa lander concept. Similar to the lunar robotic landers, the vehicle uses a single solid rocket motor to perform a braking burn as it approaches the planetary moon. The motor is jettisoned once the burn is complete. Similar to the robotic lunar missions, this vehicle also has a multiple powered phases before landing. At approximately 5 km above the surface, after the motor separates, the vehicle starts the landing site correction phase, where it targets a vertical and horizontal velocity of 100 m/s and 0 m/s respectively at 2 km altitude. At that point, the second powered phase is initiated where the Hazard Detection and Avoidance and Science Detection and Correction occurs. The vehicle targets 20 m altitude with 1 m/s vertical and 0 m/s horizontal velocity. The final sky-crane phase, similar to MSL, lowers the 300 kg (200kg descent stage and 100 kg lander) vehicle to the surface and

flies away. While the Europa lander mission has identified the sensors and performance criteria needed to achieve 100 m landing precision, SPLICE is also considering the concept of operations to identify commonalities with the other mission concepts.

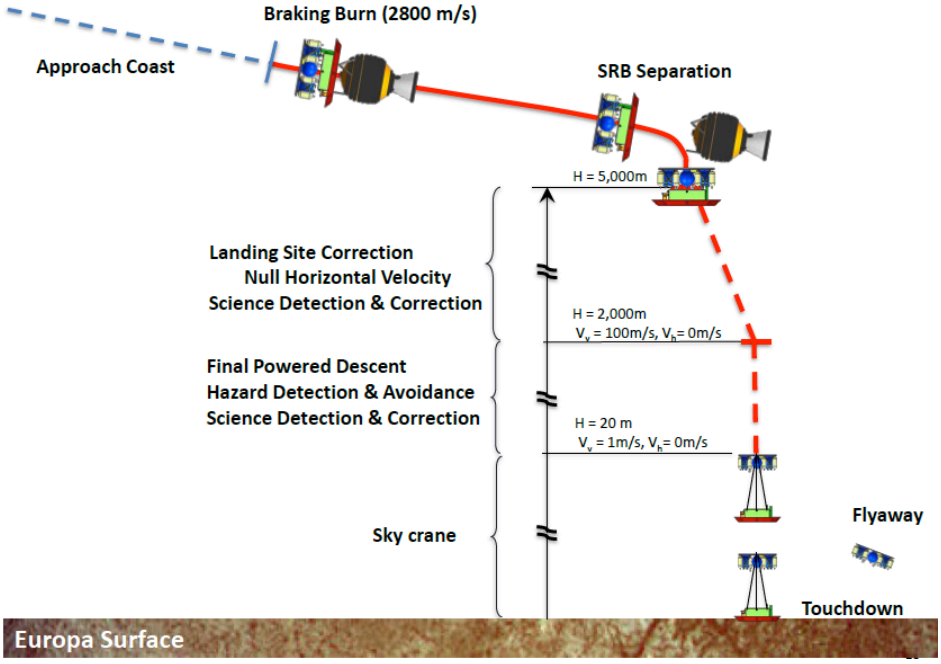

Figure 7. Europa Lander concept of operations. [14]

G. Reference Trajectories

Nominal profiles for each concept of operations are simulated using the Program to Optimize Simulated Trajectories (POST2) [15]. A similar framework is established for all concept of operation simulations such that sensor models can be easily implemented and evaluated. Initial comparisons of trajectory parameters are provided here. One set of parameters, important to precision landing are slant range and slant angle. Slant range is defined as the distance from the vehicle center of gravity to the target landing location. The slant angle is the angle between the horizontal plane containing the landing target and the slant range. Figure 8 illustrates these parameters. Slant ranges of 1000 m and 500 m are indicated with a square and a circle, respectively, on the reference trajectory plots. Sensors that measure relative quantities, like terrain relative navigation, require constrains on slant range and angle, and vehicle vertical and horizontal velocity to operate effectively. Due to the unique and yet-to-be-defined vehicle configurations, other sensor considerations, such as vehicle accommodation (sensor location on the vehicle) and sensor field of view are not considered here. Reference altitude versus velocity plots for each concept of operations are shown in Fig. 9 and are expanded to show only the lowest 1 km and last 100 m/s in Fig. 10.

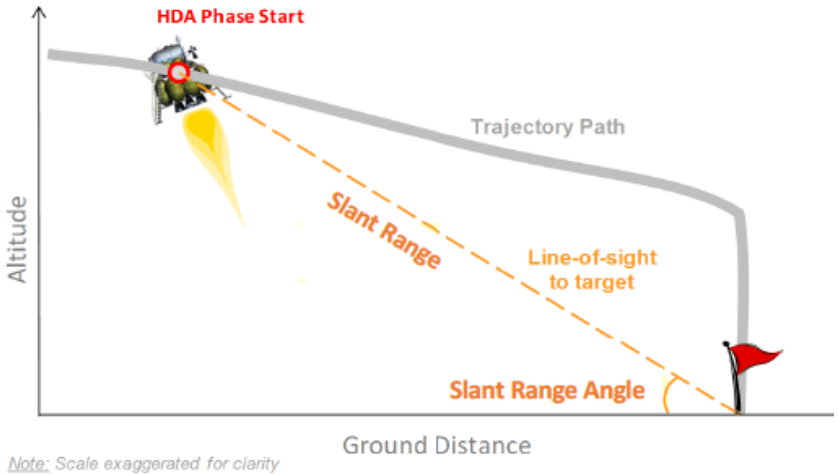

Figure 8. Definition of slant range and slant range angle.

It is important to note the low altitudes and high velocities of the human Mars mission cases (Mid and Low L/D) are due to the use of supersonic retropropulsion, which dramatically changes the trajectory geometry compared to the lunar and Europa cases and will impact sensor performance. In fact, the 1000 m and 500 m slant ranges for the Mid L/D occur while the vehicle is traveling faster than 100 m/s (off to the right of Fig. 10). The high velocities result in blurring images. Therefore, the human Mars concepts of operation may require additional sensors such as orbiting assets and surface beacons, which are also included in the sensor trade.

In addition to altitude and velocity, other trajectory parameters important to PL&HA sensor measurements include the time to image the site, or time to touchdown. Figure 11 shows the vehicle velocity versus time to touchdown for each nominal concept of operations. Note that at 500 m slant range, the lunar human and robotic mission trajectories (denoted as Altair and Merriam, respectively) have the longest time to touchdown (almost 80 s). This is by design and based on past lunar mission experience. The Mars robotic trajectories (MSL is shown here) was not attempting to perform a precision landing. Likewise, the human Mars mission cases were designed to minimize propellent, and were not redesigned to support traditional PL&HA sensor requirements.

For optimal performance, slant range angle should be greater than 60 deg. Slant angle is shown in Fig. 12. Again, for the lunar and Europa cases, the trajectories spend at least 40 seconds (and for some, as much as 80 s), at slant range angles greater than 60 deg, whereas the human Mars cases (Mid and Low L/D) spend less than 20 seconds with slant range angles in the acceptable range to achieve images of the surface to perform precise and safe landing.

These plots highlight the difference in landing philosophies (achieving PL&HA vs. minimizing propellant). The screening process will be performed on the concepts defined in the previous sections and much work remains to balance various navigation sensor requirements with the trajectory guidance and control design to achieve the highly constrained landing precision criteria with reasonable propellant use.

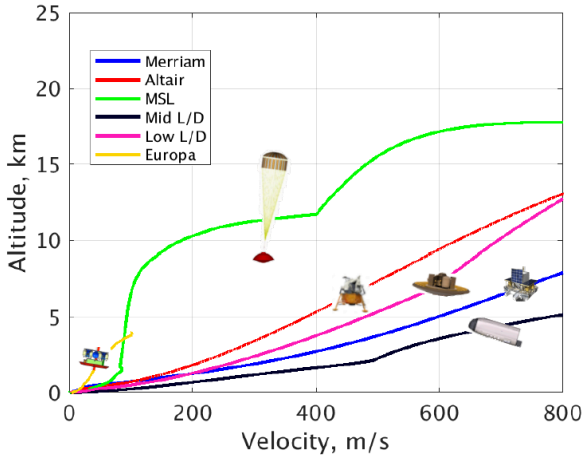

Figure 9. All concepts of operations considered; altitude versus velocity.

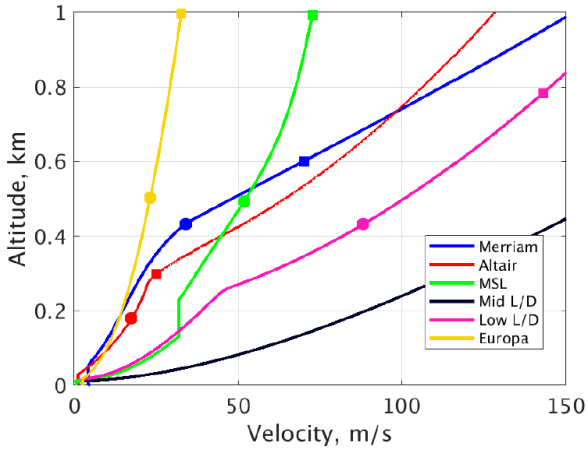

Figure 10. All concepts of operations considered; altitude versus velocity expanded. Squares =1000 m slant range, circles=500 m slant range.

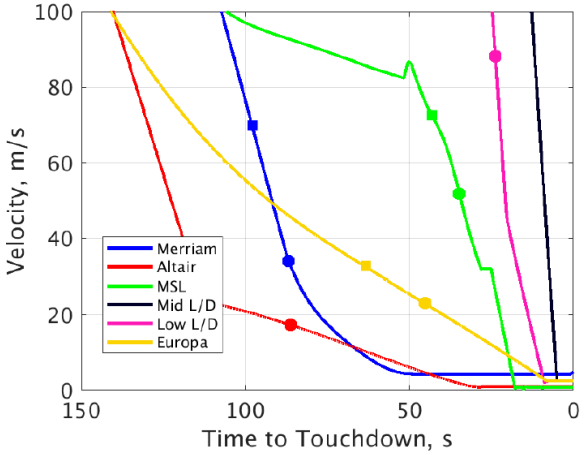

Figure 11. Vehicle velocity vs. time to touchdown.

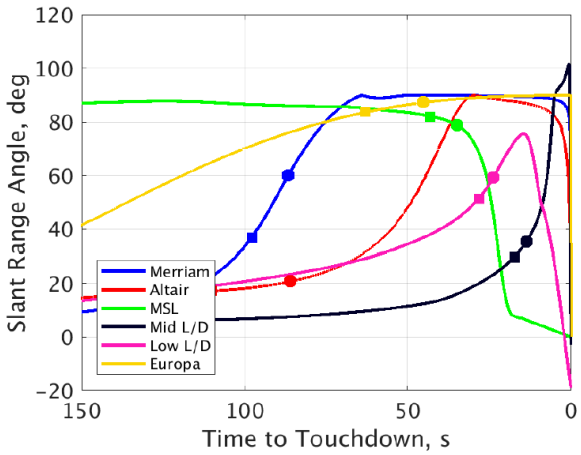

Figure 12. Slant range angle vs. time to touchdown.

III. Navigation Sensors

In addition to defining reference concept of operations, sensor models and performance definitions have been identified. Many sensors have been used on past missions or are based on recent technology development activities. Sensors considered in the PL&HA matrix requirement definition assessment include inertial measurement units (IMU), star trackers, altimeters, velocimeters, terrain relative navigation (TRN), cameras, orbiting beacons, surface beacons, air data systems, and earth-based ground updates. Each of the sensors is further classified as having low, medium and high fidelity. The sensor fidelity can represent cost, reliability, accommodation difficulty, heritage, computation level, etc. and allows for trades on these parameters. For the initial assessment a simple weighting classification was used: a rank of three represents the *highest* quality, most expensive sensor; a rank of two defines a *medium* quality sensor; a rank of one represents a *low*-quality sensor; and a rank of zero means the sensor was not considered as part of the suite assessment and has no cost. Therefore, sensor suites that satisfy top-level mission requirements are ranked according to their total cost where the smallest numbers represent the lowest cost or *best* cases. Table 2 provides the list of sensors with rank specifications. These values will continue to be refined as sensor technologies mature.

Table 2. Sensor specifications.

Sensor	Measurement	Sensor Measurement Performance Quality (3σ)		
Type	**Type**	**Low**	**Medium**	**High**
IMU (Accel/ Gyros)	Lander non-gravitational accelerations and body angular rates	Accel Velocity random walk (VRW) / Bias: 105 micro-g / 900 micro-g Accel Scale Factor: 900 ppm Accel Non-ortho: 20 arcsec Gyro ARW / Bias: 0.21 deg/sqrt(hr) / 0.3 deg/hr Gyro Scale Factor: 100 ppm Non-orthogonality: 60 arcsec	Accel VRW / Bias: 150 micro-g / 300 micro-g Accel Scale Factor: 525 ppm Accel Non-ortho: 45 arcsec Gyro ARW / Bias: 0.018 deg/sqrt(hr) / 0.15 deg/hr Gyro Scale Factor: 15 ppm Non-orthogonality: 75 arcsec	Accel VRW / Bias: 0.0003 m/s/sqrt(s) / 84 micro-g Accel Scale Factor: 450 ppm Accel Non-ortho: 17 arcsec Gyro ARW / Bias: 0.015 deg/sqrt(hr) / 0.036 deg/hr Gyro Scale Factor: 27 ppm Non-orthogonality: 19 arcsec
Star Tracker	Lander inertial-to-body attitude quaternion	Bore/Cross-sight Noise = [207,49] arcsec Misalignment = 12 arcsec	Bore/Cross-sight Noise = [68.2, 8.4] arcsec Misalignment = 0.15 deg	Bore/Cross-sight Noise = [24, 3] arcsec Misalignment = 8 arcsec
Altimeter (Slant Range)	Range to planet surface	Noise/Bias: 10 m / 100 cm Misalignment / Scale factor: 0.3 deg / 15 ppm Min/Max altitude: 100 m/ 10 km	Noise/Bias: 5 m / 50 cm Misalignment / Scale factor: 0.03 deg / 10 ppm Min/Max altitude: 50 m/ 20 km	Noise/Bias: 2.1 m/30 cm Misalignment/Scale factor: 0.003 deg / 5 ppm Min/Max altitude: 10 m / 50 km
Velocimeter	Range-rate to planet surface	Noise/Bias: 10 cm/s and 100 mm/s Misalignment / Scale factor: 0.3 deg / 15 ppm Min/Max altitude: 100 m/ 3 km	Noise/Bias: 5 cm/s and 10 mm/s Misalignment / Scale factor: 0.03 deg / 10 ppm Min/Max altitude: 50 m/ 5 km	Noise/Bias: 1.7 cm/s and 1 mm/s Misalignment/Scale factor: 0.003 deg / 5 ppm Min/Max altitude: 30 m/ 10 km
Terrain Relative Navigation	Relative position to surface features	Noise/Bias: [100 , 75, 75] m / 50 m Lat/Lon map bias: 1.0 mdeg FOV: 30 deg Min/Max Altitude: 30 m / 10 km	Noise/Bias: [75, 50, 50] m / 25 m Lat/Lon map bias: 0.5 mdeg FOV: 45 deg Min/Max Altitude: 30 m / 15 km	Noise/Bias: [40 , 25, 25] m / 15m Lat/Lon map bias: 0.3 mdeg FOV: 60 deg Min/Max Altitude: 30 m / 20 km
Terrain Camera	Relative bearing angles to surface features	Close Range Angle (Az/El) Noise: [0.05, 0.05] deg Angle (Az/El) Bias: [0.5, 0.5] deg Misalignment: 0.5deg FOV: 120 deg # of Features / Feature Bias: 4 / 20 m Min/Max altitude: 100 m / 2 km	Medium Range Angle (Az/El) Noise: [0.005, 0.005] deg Angle (Az/El) Bias: [0.2, 0.2] deg Misalignment: 0.2 deg FOV: 60 deg # of Features / Feature Bias: 7 / 15 m Min/Max altitude: 100 m / 10 km	Far Range Angle (Az/El) Noise: [0.001, 0.001] deg Angle (Az/El) Bias: [0.1, 0.1] deg Misalignment: 0.1 deg FOV: 20 deg # of Features / Feature Bias: 10 / 10 m Min/Max altitude: 100 m / 100 km
Orbiting Beacons	Range and range-rate to orbiting assets	One Beacon Range noise /bias: 50 m / 50m	Three Beacons Range noise /bias: 25 m / 25m	6 Beacons Range noise /bias: 10 m / 10m Range-rate noise/bias: 10 mm/s and 10 mm/s

		Range-rate noise/bias: 50 mm/s and 50 mm/s Orbital altitude: 10,000 km Downrng/Crosstrk/Alt Position: [1000, 750, 750] m	Range-rate noise/bias: 25 mm/s and 25 mm/s Orbital altitude: 20,000 km Downrng/Crosstrk/Alt Position: [500, 100, 100] m	Orbital altitude: 30,000 km Downrng/Crosstrk/Alt Position: [200, 50, 50] m
Surface Beacons	Range and range-rate to surface assets	One Beacon Range noise /bias: 30 m / 15m Range-rate noise/bias: 15 mm/s and 15 mm/s Min/Max range: 250 m / 15 km Beacon distance from landing site: 25 m	Four Beacons Range noise /bias: 10 m / 10 m Range-rate noise/bias: 5 mm/s and 5 mm/s Min/Max range: 100 m / 10 km Beacon distance from landing site: 100 m	10 Beacons Range noise /bias: 5 m / 5 m Range-rate noise/bias: 1 mm/s and 1 mm/s Min/Max range: 50 m / 50 km Beacon distance from landing site: 1 km
Ground Updates	Lander Inertial position velocity state	UVW Pos = [0.90, 30.05, 3.07] km UVW Vel= [28.54, 0.85, 0.15] m/s	UVW Pos = [0.15, 4.51, 0.61] km UVW Vel= [4.57, 0.14, 0.03] m/s	UVW Pos = [0.03, 0.26, 0.21] km UVW Vel= [0.24, 0.03, 0.01] m/s
Air Data Systems	Rel vel, dyn pressure, alpha/beta angles	MSL (3 transducers)	MSL (5 transducers)	MSL (10 transducers)

Evaluation of the total number of sensor combinations would require 786,432 runs (i.e. 3 (IMU) x 4 (Star Tracker) x 4 (Altimeter) x 4 (Velocimeter) x 4 (TRN) x 4 (Terrain Camera) x 4 (Orbiting Beacons) x 4 (Surface Bacons) x 4 (Ground Updates) x 4 (Air Data Systems)). However, running all the cases is computationally prohibitive, especially the high fidelity 6DOF POST2 simulation. This issue was addressed in two ways. First, a subset set of runs is selected to inform specific suite attributes. Since the first concept of operations considered lunar robotic missions and did not include an atmosphere, the Flush Air Data System was not considered. However, a model is being developed for the 6DOF simulation and will be included in the Mars concept of operations evaluation. A summary of the model is provided in Ref [16]. Likewise, orbiting assets and surface beacons are not required for the lunar robotic mission and so were not considered in the initial evaluation. Table 3 summarizes the four subsets of cases selected for the initial screening. Set #1 served to evaluate PL&HA performance without relative sensor measurements, characterizing precision landing without provisions for safety. Set #2 evaluates the full set of relative sensor qualities and types to get a more complete representation of the sensors needed without running the full factorial of cases. Set #3 was specifically selected to evaluate the effect of the timing for receiving Deep Space Network ground updates. Finally, set #4 evaluated IMU quality in the presence of a "low" quality relative sensor suite. The purpose of Set #4 was to evaluate a trade in sensor development, namely, to determine if it was more effective to invest in a single high quality IMU or a lower quality relative sensor suite which included altimeter, velocimeter and Terrain Relative Navigation (TRN). In all, this pared down the total number of runs from nearly 800,000 to a more reasonable 154 cases to inform the PL&HA matrix requirements definition.

Table 3. Sensor suite selection.

SENSOR	SET #1				SET #2				SET #3				SET #4			
	No Rel Sensors				Rel Sensor Quality				Ground Quality				IMU Quality			
	Low	Med	High	None	Low	Med	High	None	Low	Med	High	None	Low	Med	High	None
IMU	x	x	x		x				x				x	x	x	
Star Tracker	x				x				x				x			
Ground Update	x	x			x	x			x	x	x	x	x	x		
Altimeter				x	x	x	x	x	x				x			
Velocimeter				x	x	x	x	x	x				x			
TRN				x	x	x	x	x	x	x			x	x		
Total Runs	6				128				8				12			
	154 Total Runs															

The second approach to evaluating the large number of suite combinations was to use two screening tools that make assumptions about error propagation that enable the trajectories to run more quickly. These tools determined the sensor combinations that meet the defined PL&HA requirements. Only the top "best" performing suites would be included in the 6DOF simulation. The two screening tools used are described in the next section. Future work will use

the requirements matrix results to derive general navigation performance and sensor specific requirements that will impact sensor design and development.

IV. Screening Tools

The SPLICE oncept of operations studies leverage three simulation and analysis toolsets, along with PL&HA and EDL expertise from across the agency. The toolsets are LinCov (Linear Covariance) [17], New Statistical Trajectory Estimation Program (NewSTEP) [18] and POST2 (Program to Optimize Simulated Trajectories II). LinCov and NewSTEP are powerful tools for conducting rapid architectural trade studies of sensor selection, quality, and phasing during EDL to determine design points to consider in higher-fidelity, computationally expensive POST2 Monte Carlo simulations. Details of LinCov and NewStep are provided below. POST2 is a high-fidelity 6DOF simulation tool, described in the previous section, for conducting detailed analyses of atmospheric ascent and entry flight. These tools are used in complementary ways to provide a complete and thorough approach to EDL mission studies, and their independent results provide valuable cross comparisons and validation of performance against anticipated mission requirements. LinCov and NewSTEP are well-suited to quickly analyzing a large combination of sensors and sensor performance, the results of which are used to select a subset of cases for more detailed analyses within POST2 simulations. POST2 includes detailed GN&C models and algorithms and solves the full equations of motion, whereas LinCov and NewSTEP uses a linearization assumption to propagate states.

A. Linear Covariance

The first approach uses linear covariance (LinCov) analysis to determine both the navigation estimation performance along with the anticipated trajectory dispersions in a single simulation run. This approach provides the framework to quickly and reliably derive navigation requirements and evaluate various sensor suites in context of top-level mission constraints by mapping navigation errors to corresponding trajectory dispersions. Linear covariance analysis uses the non-linear system dynamics models and GN&C algorithms to generate a nominal reference trajectory which is then linearized to propagate, update, and correct an onboard navigation covariance matrix and an augmented state covariance matrix. These covariance matrices contain the statistical information comparable to that produced by Monte Carlo analysis but can be generated in a fraction of the time. Linear covariance analysis techniques have been adopted and are becoming more widely used for an assortment of aerospace applications including EDL, ascent, rendezvous and docking, on-orbit operations, and interplanetary missions.

B. NewSTEP

The second approach, NewSTEP, is a nonlinear MATLAB-based Iterative Extended Kalman Filter-Smoother (IEKFS) code designed for solving post-flight trajectory reconstruction problems using a variety of sensors, typically including on-board instrumentation and ground-based measurements. NewSTEP has been applied to a wide variety of launch vehicle and entry vehicle flight test data analysis problems including Mars EDL trajectory and atmosphere reconstruction [19]. NewSTEP typically operates in a forward filter and backward smoother step to solve a fixed-interval smoothing problem, however it can run in forward filter mode only. In this mode, NewSTEP can be configured to mimic an on-board internal navigation system that would integrate IMU data and provide measurement updates from systems such as radar altimeters using an optimal filter. NewSTEP provides a nonlinear navigation error estimate by integrating simulated sensor data along the trajectory. NewSTEP also produces an estimate of the state covariance as computed by the Kalman filter. NewSTEP can be run in a Monte Carlo mode to produce a nonlinear error analysis, or it can also be configured for linear analysis by integrating the states along a nominal trajectory and producing an estimate of the error based on the filter covariance matrix. NewSTEP has been configured in the linear covariance analysis mode for the preliminary sensor screening.

The advantages of using two methods are increased confidence in performance results, detecting and isolating simulation and algorithm defects, and additional mature analysis resources for extensive trade studies. Given the modeling complexity associated with entry, descent, and landing while incorporating a closed-loop GN&C system, having independent simulation environments ensures accuracy of performance results and prevents critical errors from lingering in the system undetected, skewing critical design decisions. The extensive scope of the SPLICE project also benefits by having additional complementary tools able to provide analysis support to explore the various trade studies of interest.

The 154 cases identified in Table 3 were initially run using the LinCov tool that allowed for screening the select cases using the robotic lunar reference trajectory concept of operations and the sensor definitions from Section III. The results are provided in Section V.

V. Results: Robotic Lunar Lander

The initial requirements matrix was developed using a LinCov tool and reference concept of operations for the Merriam robotic lunar lander described in Section II. As depicted in Fig. 13, the nominal landing scenario starts approximately one hour prior to deorbit insertion.

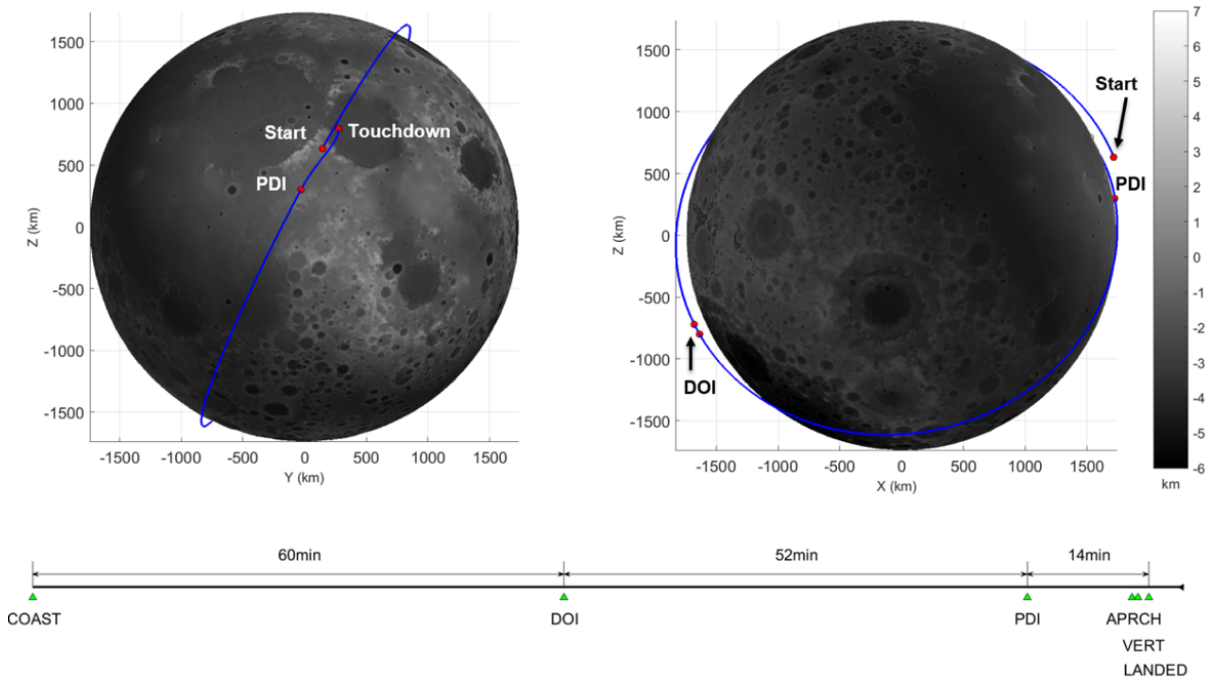

Figure 13. Simulated robotic lunar lander scenario.

The initial condition uncertainty of the vehicle's state is consistent with the Deep Space Network lunar navigation accuracy. Assuming a 1 to 2 orbit solution (3σ), the total position error at simulation initiation in x, y and z are 3.0, 5.0, and 1.0 km respectively. The velocity errors in the corresponding axes are 0.1, 0.2 and 0.05 m/s. For the initial screening effort, the study assumes no disturbance accelerations (i.e. process noise) or maneuver execution errors.

The LinCov tool was used to analyze the robotic lunar trajectory using the four sensor sets, 154 selected sensor suites combinations in all, as identified in Table 3. Figure 14 shows the touchdown position and velocity results for all 154 cases. Many of the cases do not fall within the solid red ellipse that represents the landing requirements. Thirty-three cases met all the top-level mission requirements summarized in Section II with two sensor suites having the same minimum cost. The two lowest cost sensor suites included low quality IMU, star tracker, and a medium quality DSN update along with either a *low quality velocimeter* and *medium quality TRN* (case #114r ('r' for relative sensors) - shown in blue in Table 4) or a *high quality TRN* (case #127 - shown in green in Table 4).

Many of the *high*-quality sensor specifications represent potential capability or ambitious performance levels. Based on these preliminary results, the option that has practical application to support precision landing requirements includes a *low quality velocimeter* and *medium quality TRN*, or case #114. It is noted that top-level performance requirements (excluding redundancy and backup requirements) can be satisfied without an altimeter if using TRN and velocimeter sensors. This emerging observation will be validated using NewSTEP and the POST2 simulation.

Table 4. Lowest Cost Sensor Suites.

Sensor	Low	Med	High	None
IMU	X			
Star Tracker	X			
Ground Update		X		
Altimeter				X
Velocimeter	X	X		
TRN		X	X	

*Gray represents models in common

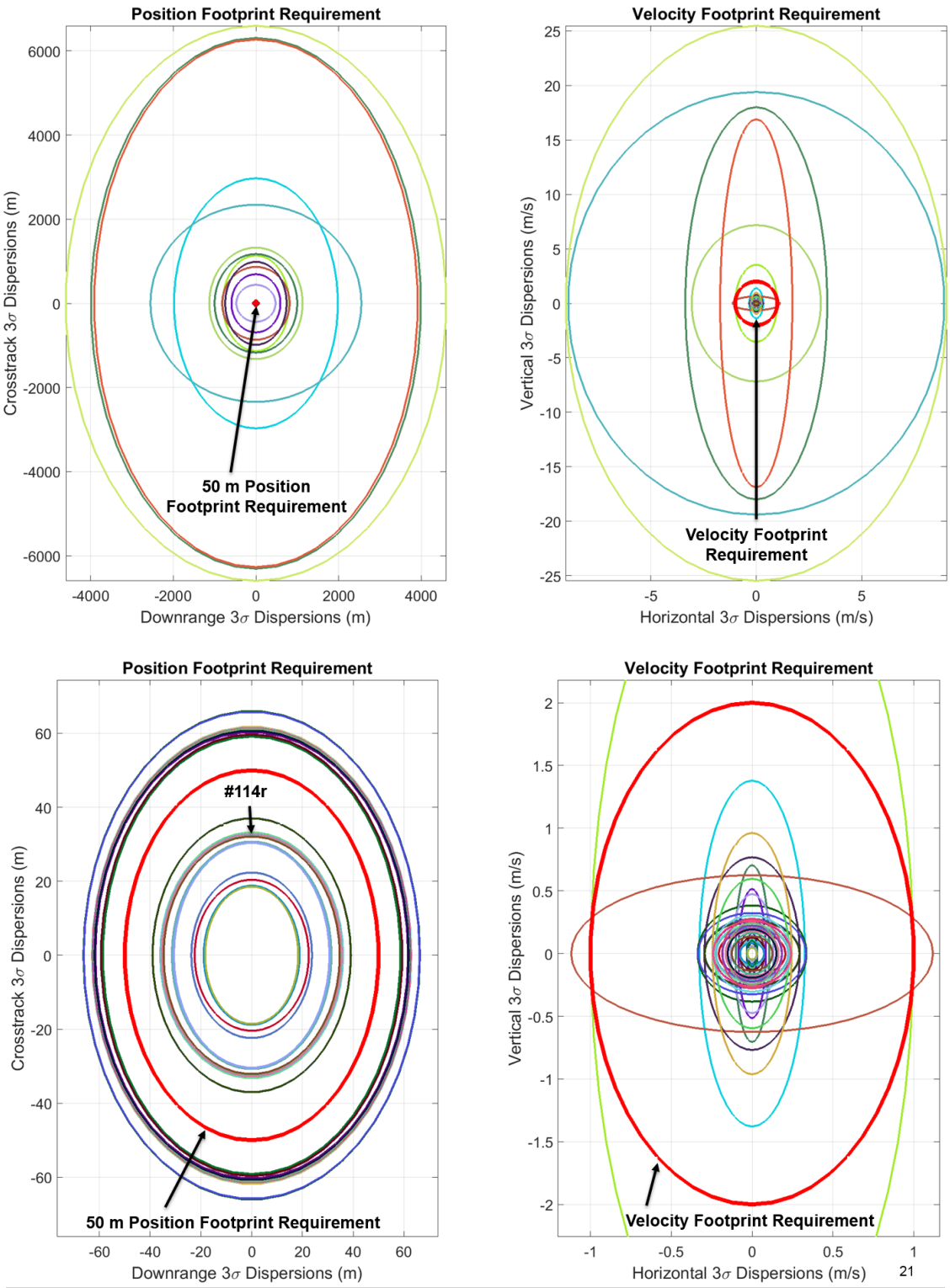

Figure 14. Touchdown relative position (left) and velocity (right) dispersions (correlations not reflected) of the 154 selected sensor suites for the lunar robotic lander concept of operations.

A. Sensor Suite Result Summary

Each of the four sets of sensor suites described in Table 3 had a particular objective. The results from the first sensor set demonstrated that precision landing requirements cannot be satisfied without relative sensors. With only an IMU, star tracker, and ground updates, footprint dispersions can be larger than 6 km (3σ) with vertical velocity dispersions at touchdown as large as 25 m/s (3σ). When a medium quality DSN ground update is incorporated with a high performing IMU, the landing footprint dispersions are potentially less than 1.5 km (3σ).

The second set identified the type and quality of relative sensors needed to support precision landing. Out of the 128 different sensor suites evaluated in this set, 28 of them satisfied requirements. These preliminary results suggest that a minimum cost sensor suite could include a *high performing TRN* sensor with an IMU, star tracker, and DSN ground update can meet PL&HA requirements. An equally low-cost sensor option could utilize a medium quality TRN sensor with a *low quality velocimeter* combined with an IMU, star tracker, and DSN ground update. These results suggest that precision landing requirements can be achieved without an altimeter, however, performance increases with its incorporation.

The third set explored the impact of the DSN ground update quality. With regards to footprint dispersions, the DSN ground update quality does not influence the performance when the relative sensors are active. However, the DSN ground update quality impacts change in velocity dispersions and propellant required to meet precision landing requirements.

The fourth and final set aimed to determine the impact of the quality of the IMU. Given the current assumptions, the quality of the IMU does not appear to have significant effects on the footprint dispersion requirements at touchdown when using a star tracker and other relative sensors such as TRN, altimeter, and velocimeter. These preliminary results suggest a low quality IMU with a star tracker is adequate when accompanied with the appropriate relative sensors.

B. Optimal Sensor Suite Results

This section highlights the particular performance of one of the low-cost *optimal sensor suite* cases and illustrates the data generated for each of the 154 test cases. The time history of the navigation performance, the resulting trajectory dispersions, and sensitivity analysis for the sensor suite #114 are shown below. This sensor suite includes a medium class terrain relative navigation (TRN) system and a low quality velocimeter along with a medium quality DSN ground update 30 min prior to deorbit burn, a low fidelity star tracker and IMU.

The altitude verses time profile for case #114 is highlighted in the lower right image of Fig. 15. The table in the upper right shows the values of the position, velocity, and attitude navigation errors at different key epochs along the trajectory. The left side of Fig. 15 shows the components of errors in position, velocity, and attitude as a function of time in minutes for the trajectory. The top and middle left most plots show the individual components of position and velocity error in UVW coordinates where U is in the radial direction, V is primarily in the vehicle's velocity direction, and W is out-of-plane or parallel to the orbital angular velocity vector. The total root sum square (RSS) of the errors is also provided.

It is notable that position and velocity errors grow during the coast phase until the DSN update which occurs 30 min prior to deorbit burn. This effectively reduces the position and velocity errors in all axes until the deorbit insertion (DOI) burn that occurs at 60 min. Burn execution errors are not modeled. Therefore, the growth in both position and velocity error after DOI comes from navigation uncertainty at the time of the burn and the errors in estimating the impulsive maneuver. During the approach phase, when TRN is active the error is again reduced to achieve precision landing constraints.

The vehicle attitude errors are not affected by the DSN update but are reduced significantly by the last measurement from the star tracker which turns off approximately 10 min prior to PDI and is improved somewhat by TRN. The drop in attitude uncertainty at PDI is due to the correlation between the TRN sensor and sensed acceleration by the IMU in the body frame (this trend in observed during ascent when GPS measurements are incorporated with accelerometer measurements). Near touchdown there is an increase in attitude errors due to the gyros responding to the control system imparting larger angular rates in the yaw axis to support the desired landing configuration.

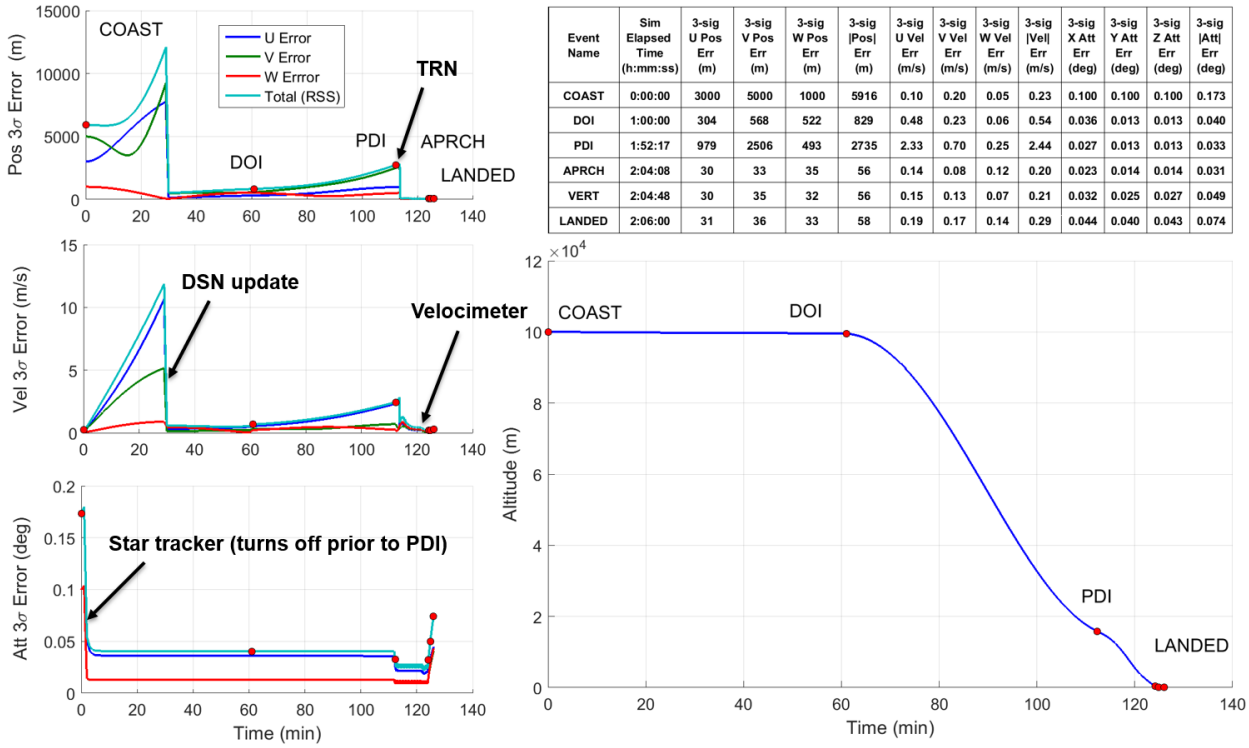

Event Name	Sim Elapsed Time (h:mm:ss)	3-sig U Pos Err (m)	3-sig V Pos Err (m)	3-sig W Pos Err (m)	3-sig |Pos| Err (m)	3-sig U Vel Err (m/s)	3-sig V Vel Err (m/s)	3-sig W Vel Err (m/s)	3-sig |Vel| Err (m/s)	3-sig X Att Err (deg)	3-sig Y Att Err (deg)	3-sig Z Att Err (deg)	3-sig |Att| Err (deg)
COAST	0:00:00	3000	5000	1000	5916	0.10	0.20	0.05	0.23	0.100	0.100	0.100	0.173
DOI	1:00:00	304	568	522	829	0.48	0.23	0.06	0.54	0.036	0.013	0.013	0.040
PDI	1:52:17	979	2506	493	2735	2.33	0.70	0.25	2.44	0.027	0.013	0.013	0.033
APRCH	2:04:08	30	33	35	56	0.14	0.08	0.12	0.20	0.023	0.014	0.014	0.031
VERT	2:04:48	30	35	32	56	0.15	0.13	0.07	0.21	0.032	0.025	0.027	0.049
LANDED	2:06:00	31	36	33	58	0.19	0.17	0.14	0.29	0.044	0.040	0.043	0.074

Figure 15. PL&HA results for case #54. Position, velocity and attitude component errors (left). Table of numerical values and flight profile (right).

Figures 16 and 17 show the trajectory dispersions during final approach and at touchdown for case #114. These results highlight the overall GN&C performance capturing the various closed-loop descent and landing guidance algorithms given the navigation performance based on the selected sensor suite. These preliminary results suggest that the final position criteria are satisfied and there is 28% margin in the landing footprint requirement and a 77% margin in the vertical and horizontal landing velocity dispersion requirement. This margin will decrease as the maneuver execution errors and system process noise are incorporated into the analysis.

Figures 18 and 19 provide the sensitivity analysis of the trajectory dispersions during final approach and touchdown for case #114. These plots emphasize the key contributors to the overall system performance and give insight to how each sensor impacts the overall system performance. For example, in Fig. 18 the in-plane trajectory dispersions prior to the approach phase are largely due to the initial condition uncertainty prior to DOI. However, as the lander starts the approach and vertical descent phase, the trajectory dispersions are dominated by the TRN sensor accuracy. In fact, the footprint dispersions at touchdown are largely due to the TRN, velocimeter, and accelerometer. The horizontal and vertical velocity dispersions at touchdown are impacted the greatest by the accelerometer measurements.

The next step in the process is to run the top cases through NewSTEP and compare the results. The sensor suite combinations that rise to the top of both screening approaches will be implemented in the POST2 6DOF simulation for extensive performance analysis using a complete set of environmental dispersions and concept of operations trades.

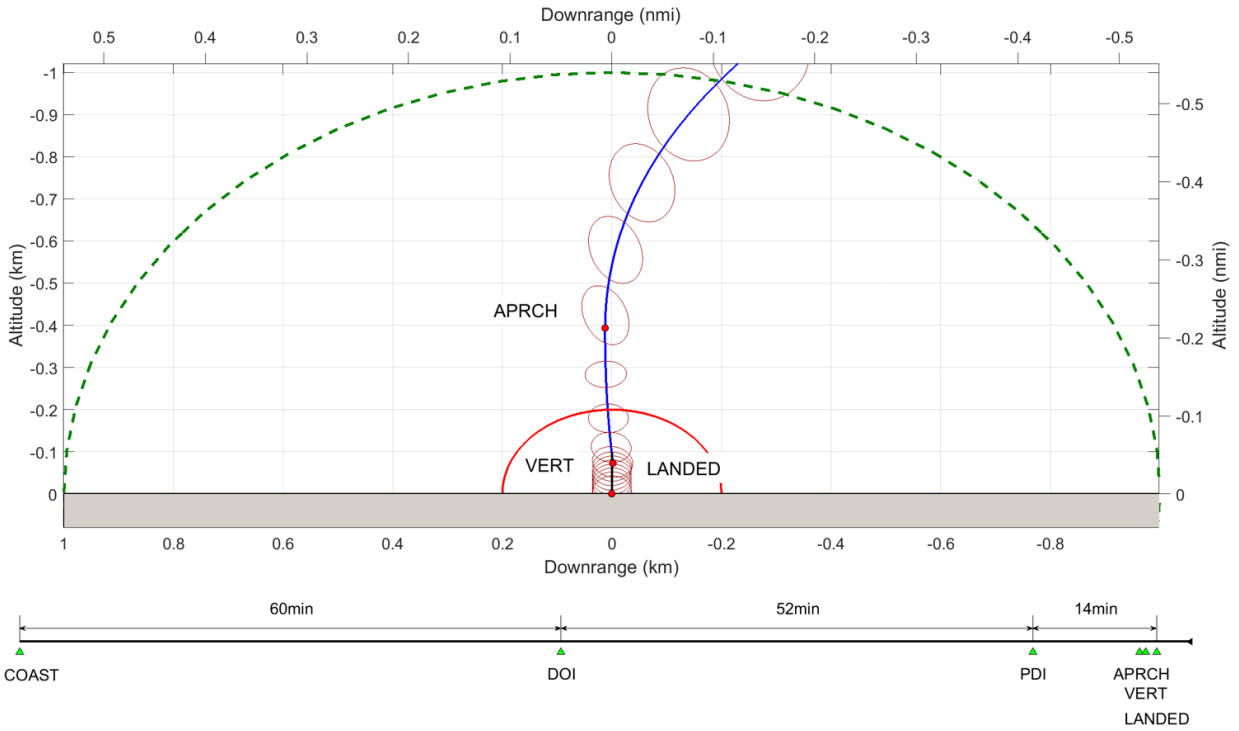

Figure 16. Case #114 down and cross range during final approach. The mission timeline is provided at the bottom of the plot.

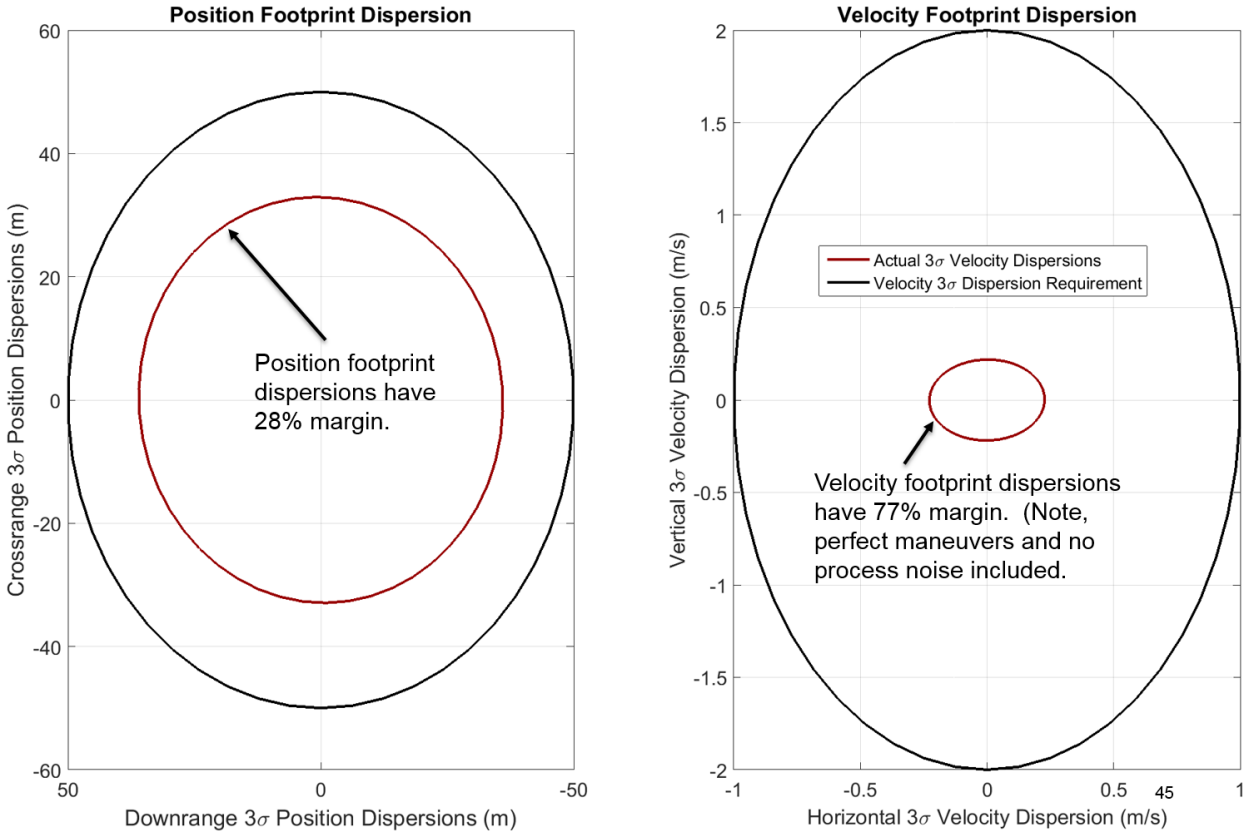

Figure 17. Case #114 down and cross range during final approach.

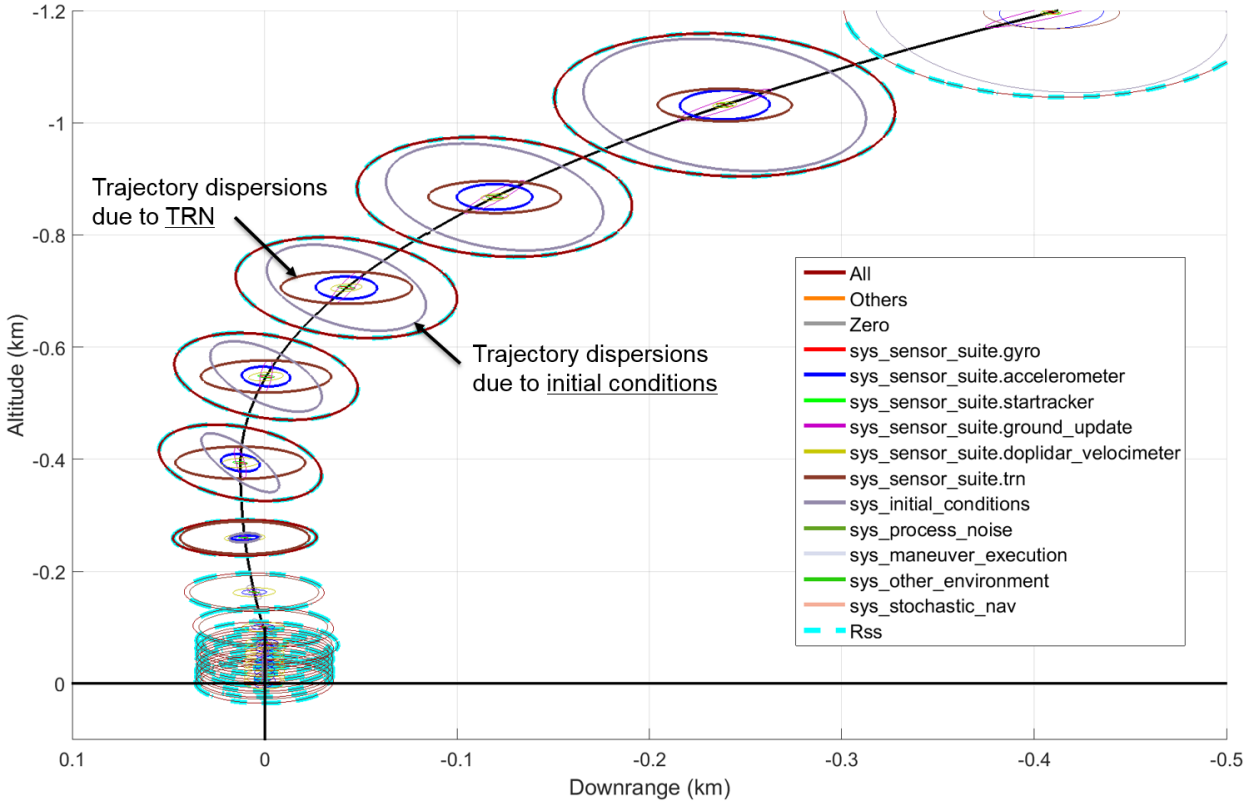

Figure 18. Case #114 sensitivity analysis results for trajectory dispersions during final approach.

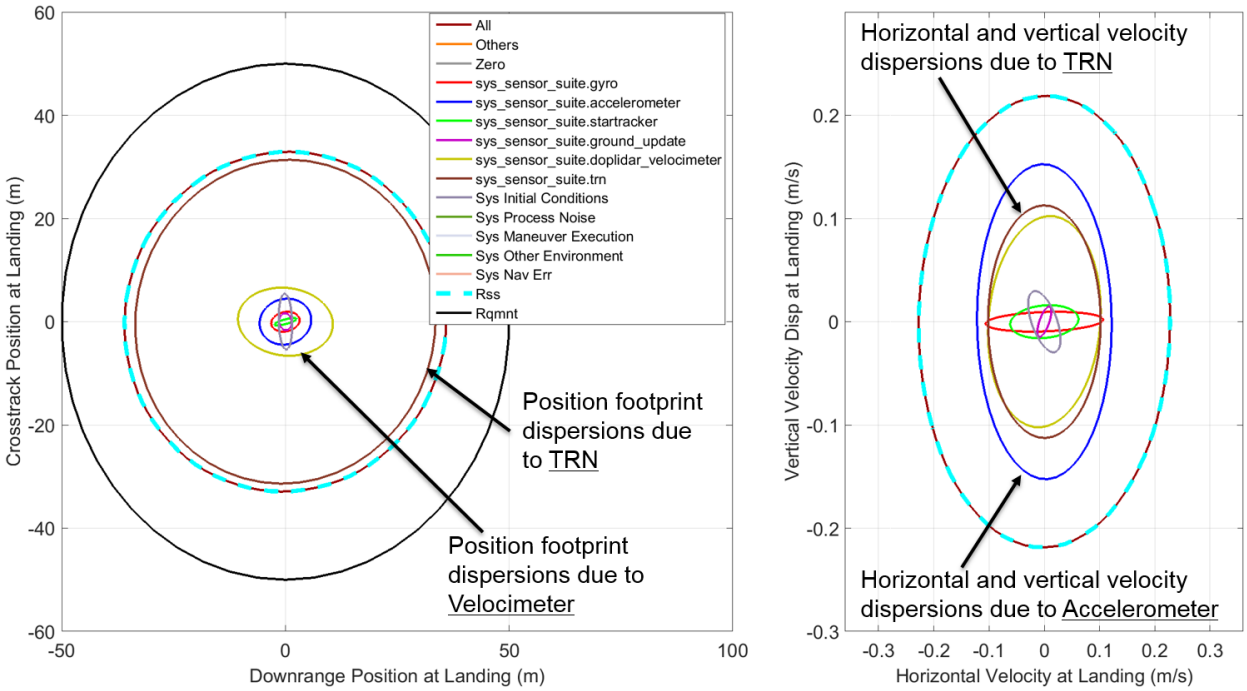

Figure 19. Case #114 sensitivity analysis results for touchdown position and velocity dispersions.

VI. Conclusion

Defining a PL&HA requirements matrix for a broad array of missions is a challenge, especially since many of the mission concepts are not well defined, nor are details available for individual mission vehicle designs. However, there is potential to identify high payoff investments by identifying PL&HA sensor elements that satisfy landing requirement for multiple missions. The matrix definition effort strives to use both medium and high-fidelity simulations to evaluate a wide range of sensor suites. Sensitivity results show that position footprint dispersions are dominated by TRN accuracy (See Fig. 19). Touchdown horizontal and vertical velocity dispersions are impacted most by velocimeter sensor and accelerometer. The initial assessment, described herein, has already identified that top-level PL&HA performance requirements (excluding redundancy and backup requirements) can be satisfied without an altimeter provided the mission has a medium class TRN and velocimeter and includes existing IMU and star tracker technologies.

Much work remains to evaluate the other concepts of operations using both LinCov and NewSTEP. The top sensor combinations that satisfy the most constraints must then be modeled in the POST2 6DOF simulation after detailed sensor models are developed and incorporated. The key outcome of this analysis will identify a common set of sensors, both type and fidelity, that satisfy a wide range of mission performance requirements. Those common elements will inform future NASA technology developments in an effort to improve vehicle PL&HA for future missions.

Acknowledgments

The authors acknowledge the very large team of individuals who, together, are supporting the SPLICE project and developing the PL&HA sensors, algorithms, software, analyses, and mission infusion pathways. The work described herein involves contributions from NASA JSC, HQ, LaRC, GSFC, JPL, and several other supporting institutions and universities. The SPLICE support from the Jet Propulsion Laboratory, California Institute of Technology, was performed under contract with the National Aeronautics and Space Administration (Government sponsorship acknowledged).

References

[1] Carson, J. M., et al. "Flight Testing ALHAT Precision Landing Technologies Integrated Onboard the Morpheus Rocket Vehicle." AIAA SPACE 31 Aug 31 to Sep 2, 2015, Pasadena, California, AIAA 2015-4417.

[2] Carson, J. M., et al. "COBALT: Development of a Platform to Flight Test Lander GN&C Technologies on Suborbital Rockets." AIAA SciTech, January 9 – 13, 2017, Grapevine, Texas, AIAA 2017-1496.

[3] Carson, J. M., Munk, M. M., Sostaric, R. R., Estes, J. N., Amzajerdian, F., Blair, B. Rutish, D. K., Restrepo, C. I., Cianciolo, A. D., Chen, G. T., Tse, T., "The SPLICE Project: Continuing NASA Development of GN&C Technologies for Safe and Precise Landing." AIAA SciTech 2019, San Diego, CA.

[4] National Academy of Sciences "Visions and Voyages for Planetary Science in the Decade 2013 to 2022" The National Academies Press, March 2011.

[5] Space Policy Directive-1, Presidential Documents, December 11, 2017; https://www.hsdl.org/?view&did=806399

[6] Sostaric, Ronald. "Powered Descent Trajectory Guidance and Some Considerations for Human Lunar Landing." AAS 07-051. 30th Annual AAS Guidance and Control Conference. Feb 3-7, 2007. Breckenridge, CO.

[7] Kos, L., Polsgrove, T., Sostaric, R., Braden, E., Sullivan, J., Le, T., "Altair Descent and Ascent Reference Trajectory Design and Initial Dispersion Analyses", AIAA Guidance, Navigation, and Control Conference and Exhibit, Toronto, Canada, August 2 –5, 2010.

[8] Davis, J. L., Striepe, S. A., Maddock, R. W., Hines, G. D., Paschall, S., Cohanim, B. E., Fill, T., Johnson, M. C., Bishop, R. H., DeMars, K. J., Sostaric, R. R., Johnson, A. E. "Advanced in POST2 End-to-End Descent and Landing Simulation for the ALHAT Project" AIAA/AAS Astrodynamics Specialist Conference and Exhibit, Aug 2008, AIAA 2008 – 6938.

[9] Way, D. W., Davis, J. L., Shidner, J. D. "Assessment of the Mars Science Laboratory Entry, Descent, and Landing Simulation." AAS 13-420.

[10] Cianciolo, A. D., Dillman, R., Brune, Lugo, R. A., Polsgrove, T. T., Percy T. K., Sutherlin, S., A., Johnson, C., and Cassell, A., "Human Mars Entry, Descent and Landing Architecture Study: Deployable Decelerators," AIAA SPACE 2018, Orlando, FL, AIAA 2018-5191.

[11] Polsgrove, T. T., Percy, T. K., Garcia, J., Cianciolo, A. D. Samareh, J., Lugo, R., Robertson, E., Cerimele, C., Sostaric, R., and Garcia, J., "Human Mars Entry, Descent and Landing Architecture Study: Rigid Decelerators." AIAA SPACE 2018, Orlando, FL, AIAA 2018-5192.

[12] C. J. Cerimele, E. A. Robertson, R.R. Sostaric (editor), J. A. Garcia, "A Rigid, Mid-Lift-to-Drag Ratio Approach to Human Mars Entry, Descent, and Landing", AIAA SciTech 2017, Grapevine, TX, Jan. 2017.

[13]Cianciolo, A. D. and Polsgrove, T. T., "Human Mars Entry, Descent and Landing Architecture Study Overview," AIAA Paper 2016-5494, Sept. 2016.

[14] Dooley, J. "Mission Concept for a Europa Mission" 2018 IEEE Aerospace Conference 10.1109/AERO.2018.8396518

[15] Striepe, S.A., et al, "Program to Optimize Simulated Trajectories (POST2), Vol. II Utilization Manual," Version 1.1.6.G, January 2004, NASA Langley Research Center, Hampton, VA.
[16] Lugo, R. et al. "Integrated Flush Air Data System Modeling for Planetary Entry Guidance with Direct Force Control" AIAA SciTech Jan 2019
[17] Woffinden, D. , Robinson S., Williams, J., and Putnam, Z "Linear Covariance Analysis Techniques to Generate Navigation and Sensor Requirements for the Safe and Precise Landing -- Integrated Capabilities Evolution (SPLICE) Project." AIAA SciTech 2019, San Diego, CA.
[18] Karlgaard, C., Tartabini, P., Blanchard, R., Kirsch, M., and Toniolo, M., "Hyper-X Post-Flight Trajectory Reconstruction," *Journal of Spacecraft and Rockets*, Vol. 43, No. 1, 2006, pp. 105-115.
[19] Karlgaard, C., Kutty, P., Schoenenberger, M., Munk, M., Little, A., Kuhl, C., and Shidner, J., "Mars Science Laboratory Entry Atmospheric Data System Trajectory and Atmosphere Reconstruction," *Journal of Spacecraft and Rockets*, Vol. 51, No. 4, 2014, pp. 1029-1047.